Journey to the center of a Schwarzschild-de Sitter black hole using quantum computing

Amy Joseph[(1)] and Michael McGuigan[(2)]
(1) Arizona State University, (2) Brookhaven National Laboratory

Summer 2021

Abstract

The intricacies and features of de Sitter space are explored using both classical and quantum computing methods. Recent cosmological measurements point to the existence of dark energy driving an exponential expansion of the Universe. One leading explanation for dark energy is the existence of a nonzero cosmological constant. If that's the case, then the solution to Einstein's equation without matter will be de Sitter space. At the same time a large amount of information is becoming available about the properties of black holes both from stellar collapse and from supermassive black holes at the center of galaxies. In this case, the solution to Einstein's equation is the Schwarzschild solution. The way to reconcile these two phenomena is through the de Sitter-Schwarzschild solution. However, there are difficulties in understanding the connection between the entropy of de Sitter space and that of black holes. In addition, it is an outstanding problem to understand the microstates whose counting could lead to this entropy. In this paper, we use quantum computing to analyze several aspects of the de Sitter-Schwarzschild solution in order to obtain a fresh perspective on this problem. We study the classical solutions for a de Sitter black hole, thermodynamics, Hamiltonian, and the thermofield double description. We also compare the results from the classical computer to the quantum computer, in order to study the abilities of the quantum computer.

1 Introduction

de Sitter (dS) space is a Lorentzian manifold defined to have positively curved spacetime with a positive cosmological constant (dark energy) and energy density. It is considered to be empty of matter - both dark and ordinary. Our Universe is spatially flat but it's curved when we include the time dimension. Despite our Universe being filled with matter, it's expanding, foreshadowing its future as a de Sitter universe [1]. This is to say, our Universe is asymptotically de Sitter. Also, de Sitter space possesses a cosmological constant which is static everywhere in the Universe (via Einstein's field equations), meaning the curvature is homogeneous throughout. In other words, de Sitter space is maximally symmetric. Particularly, de Sitter space is the maximally symmetric solution to Einstein's field equations in a vacuum with a positive cosmological constant, Λ.

One reason to study de Sitter space is the lack of references on it. Many sources have explored anti-de Sitter (adS) space, which has a negative curvature to spacetime and emerged before we knew the Universe's exponential expansion. adS is useful for understanding field theory but fails when it comes to gravity. Our dS space is indeed much more difficult but it is also more accurate, which is why it's crucial to understand.

There are several parallels that can be drawn between features of the de Sitter black hole and the Universe, making them excellent concepts to study in tandem. The Universe's cosmological horizon is similar to the event horizon of a black hole, in that they both possess temperature and entropy. Therefore, if the Universe is truly de Sitter, one can apply the quantum properties of black holes to our Universe [2]. This creates the Schwarzschild-de Sitter spacetime - the focus of this paper.

2 Classical Solutions for de Sitter Black Holes

The main difference between Schwarzschild-de Sitter (SdS) and de Sitter or Schwarzschild space alone, is that SdS has two event horizons - the black hole horizon and the cosmological horizon - whereas the theories apart only have one [3].

To reiterate the key point from the introduction, de Sitter spacetime is the maximally symmetric solution to Einstein's vacuum field equation using a positive dark energy value, Λ. By definition, maximally symmetric describes a space which is both homogeneous and isotropic. Here, we will explore the classical Schwarzschild-de Sitter (SdS) solutions to Einstein's equation. The SdS metric can be derived by starting with the Schwarzschild metric,

$$ds^2 = -f\left(r\right)dt^2 + \frac{dr^2}{f\left(r\right)} + r^2\left(d\theta^2 + \sin^2\theta d\phi^2\right)$$

And the solutions for Einstein's field equation in a vacuum, where M is the mass of the black hole,

$$f_{bh}\left(r\right) = 1 - \frac{2M}{r}$$
$$f_c\left(r\right) = 1 - \Lambda r^2$$
$$f\left(r\right) = 1 - \frac{2M}{r} - \Lambda r^2$$

In which, $f_{bh}(r)$ represents a black hole in empty spacetime with stress-energy = 0, and $f_c(r)$ represents a positive Λ de Sitter space with stress-energy = 3Λ. Thus, $f(r)$ is simply a superposition of these solutions, generating the SdS solution. We can then apply this summation to the above metric to create the SdS metric,

$$ds^2 = -\left(1 - \frac{2M}{r} - \frac{r^2}{l^2}\right)dt^2 + \left(1 - \frac{2M}{r} - \frac{r^2}{l^2}\right)^{-1}dr^2 + r^2\left(d\theta^2 + d\phi^2\sin^2\theta\right)$$

Note that we're working in $D = 3 + 1$ dimensions - we need 4 dimensions for a dS black hole to exist. When we use the generic $f(r)$ function in the metric,

$$ds^2 = -f(r)dt^2 + f(r)^{-1}dr^2 + r^2\left(d\theta^2 + d\phi^2\sin^2\theta\right)$$

we can derive the Ricci scalar for the metric using Mathematica, resulting in,

$$R = -\frac{-2 + 2f(r) + 4rf'(r) + r^2f''(r)}{r^2}$$

Which is what we expect to see.

3 Entropy

Despite black holes being regions of spacetime, not objects, they still possess thermodynamic properties (entropy and temperature) when studied quantum mechanically. Hawking and Gibbons showed that this also applied to cosmological event horizons. In this section, the thermodynamics of the Schwarzschild-de Sitter (SdS) black hole and the Universe are explored and compared. The following entropy derivations are referenced from [3].

The radius equations for the SdS black hole event horizon and the cosmological horizon are as follows,

$$r_{bh} = \frac{2M}{\sqrt{3y}} \cos\left(\frac{\pi + \psi}{3}\right)$$

$$r_c = \frac{2M}{\sqrt{3y}} \cos\left(\frac{\pi - \psi}{3}\right)$$

where $y = \frac{M^2}{l^2}$, $l = \frac{\sqrt{\Lambda}}{3}$, and $\Psi = \cos^{-1}(3\sqrt{3y})$. Note that as y approaches zero, the black hole's event horizon radius approaches twice the mass, M, while the cosmological event horizon radius approaches l.

Next, the surface gravity equation for each horizon is given by,

$$k_{bh} = \alpha \left| \frac{M}{{r_{bh}}^2} - \frac{r_{bh}}{l^2} \right|$$

$$k_c = \alpha \left| \frac{M}{{r_c}^2} - \frac{r_c}{l^2} \right|$$

where

$$\alpha = \frac{1}{\sqrt{1 - (27y)^{\frac{1}{3}}}}$$

Note here that as y approaches zero, the black hole's surface gravity approaches $\frac{1}{4M}$ and the cosmological horizon's surface gravity approaches $\frac{1}{l}$.

Finally, the entropy equation for SdS is essentially the summation of each individual entropy plus an extra term,

$$S_{SdS} = \frac{\pi}{{k_{bh}}^2} + \frac{\pi}{{k_c}^2} + \frac{2\pi}{k_c k_{bh}}$$

From here, we plot the total entropy of the system, S_{SdS}, as a function of mass, M, with $l = 1$ in Figure 1.

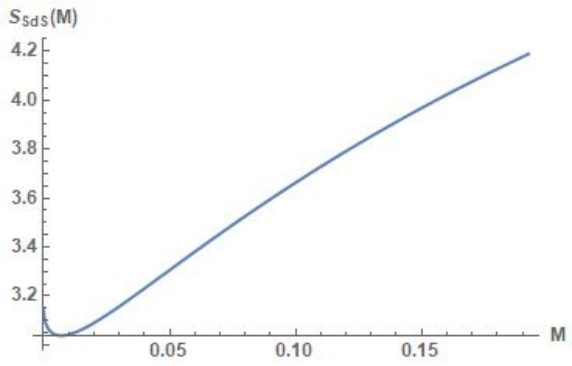

Figure 1: Plot of the total entropy of the system as a function of mass. Note the decrease in the entropy for small mass, $0 < M < 0.007$.

Next, we plot the surface gravity of each as a function of mass, again with l set to 1.

Another set of equations that describes the entropy of each piece of the system is given by [4],

$$S_{bh} = \frac{A_{bh}}{4} = \pi {r_{bh}}^2$$

$$S_c = \frac{A_c}{4} = \pi {r_c}^2$$

Which can then be added together to create the total entropy of the system,

$$S = S_{bh} + S_c$$

We can plot the two entropies separately to establish a comparison, seen in Figure 2.

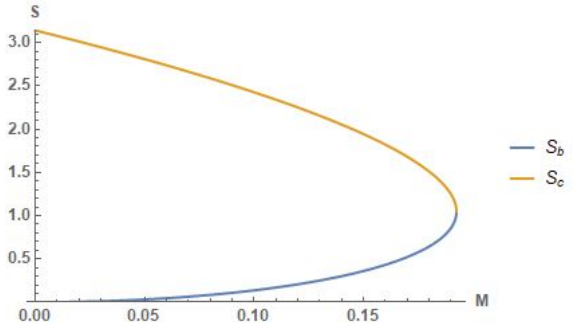

Figure 2: Plot of each entropy, S_{bh} and S_c, separately as a function of mass. Notice the point of intersection, $M = \sqrt{\frac{1}{27}}$.

Again, there is an interesting convergence point at $M = \sqrt{\frac{1}{27}}$. This is the Nariai limit (or Nariai black hole), which we will discuss in the next section.

Temperature is another property the two event horizons have that is important to study. The equation is as follows,

$$\beta = T^{-1} = \frac{\partial S}{\partial M}$$

We can derive the black hole entropy, S_b, and the cosmological entropy, S_c and then plot the temperatures as functions of mass (Figures 3 and 4).

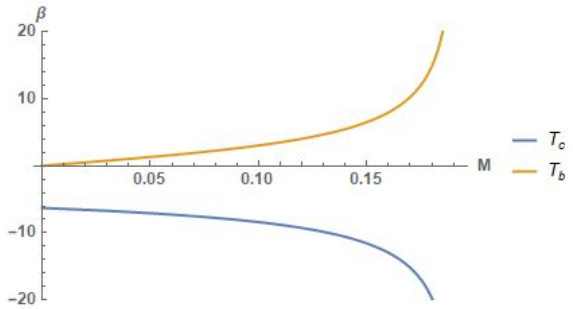

Figure 3: Plot of the inverse temperature as a function of mass. The cosmological temperature is in blue and the black hole temperature is in orange.

Notice how the cosmological temperature tends toward negative infinity (the Big Chill) and the black hole temperature tends toward positive infinity.

The asymptotes show the effect of the black hole on the de Sitter horizon as well as the effect of the cosmological constant on the black hole horizon. The black hole

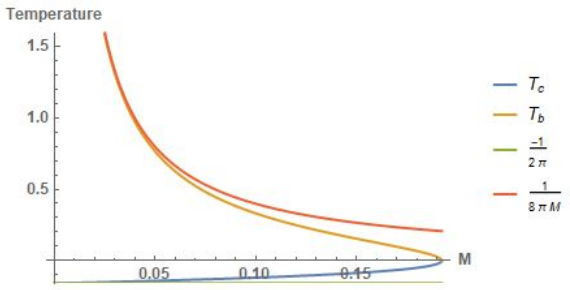

Figure 4: Plot of the temperature as a function of mass. The cosmological temperature is in blue and the black hole temperature is in orange. Their respective asymptotes are in green and red.

makes the de Sitter temperature decrease in absolute value while the cosmological constant makes the black hole temperature decrease.

4 Nariai Limit

An important solution to study is the Nariai black hole. Its event horizon approaches the cosmological horizon, $r_{bh} \rightarrow r_c$, so that the two radii coincide - making it the largest possible de Sitter black hole. It is virtually a Universe consisting only of the black hole, but it may be unstable. The black hole would evaporate, decreasing in mass, and the radius of the Universe would expand, so in the end all that is left is de Sitter space. This would take a considerable amount of time, though, as it is such a massive black hole.

In Figure 5, we plot the addition of the SdS black hole entropy with the cosmological entropy, along with the Nariai black hole, $S_n = \frac{2\pi}{3}$. This figure, Figure 2, and Figure 4 show that as the mass of the system (SdS black hole and Universe) increases, the entropy approaches the Nariai black hole - the maximum solution.

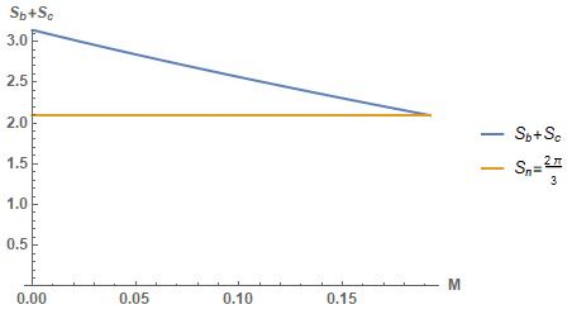

Figure 5: Plot of the sum of the SdS black hole entropy, S_b, and the cosmological entropy, S_c, as a function of the mass. S_n is the Nariai black hole solution. The plot shows the total entropy approaches the Nariai solution, until they coincide at $M = \sqrt{\frac{1}{27}}$ (the largest possible black hole mass).

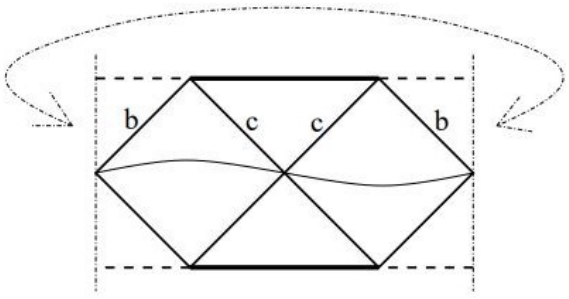

Figure 6: The Schwarzschild-de Sitter Penrose diagram from [2]. Nariai spacetime has a similar diagram, where the bounds have a different meaning. The horizons for both the black hole and the Universe are depicted by b and c, respectively. The singularity is indicated by the dashed line.

An unusual, but key feature of the Nariai black hole is that it does not have a spacial singularity. According to the Penrose diagram found in [2], shown here in Figure 6: the dashed lines are the singularity. Thus, the singularity appears to be in time rather than space.

5 The Hamiltonian and Mass Operators

The Hamiltonian is essentially the quantum version of the Friedmann equation, which describes the evolution of the Universe - making it a key piece to study.

Following the definitions and derivations of the Hamiltonian constraint and mass operator from [12] we have,

$$H_{WD} = -\frac{a}{b^2}p_a^2 + \frac{2}{b}p_a p_b + a - \lambda a b^2$$

$$2M = \frac{1}{b}p_a^2 + b - \frac{\lambda}{3}b^3$$

Using the Kronecker product to construct each quantum mechanically, we can simplify the Hamiltonian of the SdS black hole interior to the difference between two simple harmonic oscillators,

$$H_{WD} = \frac{1}{2}p_u^2 + \frac{1}{2}u^2 - (\frac{1}{2}p_v^2 + \frac{1}{2}v^2)$$

while the mass operator can be written as the sum,

$$M = \frac{1}{2}p_u^2 + \frac{1}{2}p_v^2 + \frac{1}{2}u^2 + \frac{1}{2}v^2 + p_u p_v - uv$$

It is easy to then use Mathematica to prove the commutation of the Hamiltonian with the mass operator is zero,

$$[H, M] = [HM - MH] = 0$$

Additionally, they obey the Wheeler-DeWitt equation,

$$H\,|\psi\rangle = 0$$

$$M\,|\psi\rangle = m_{bh}\,|\psi\rangle$$

We use the quantum computer (QISkit) to study the operators using the Variational Quantum Eigensolver (VQE). The VQE is essentially the variational method from quantum mechanics, in which it repeatedly modifies an ansatz for a wavefunction in an effort to get as accurate of a result as possible for the eigenvalues. In the following figures, we plot the VQE convergence for the four different optimizers utilized and using 4 qubits. Each curve represents a different optimizer as they each try to produce the most accurate result for the eigenvalue.

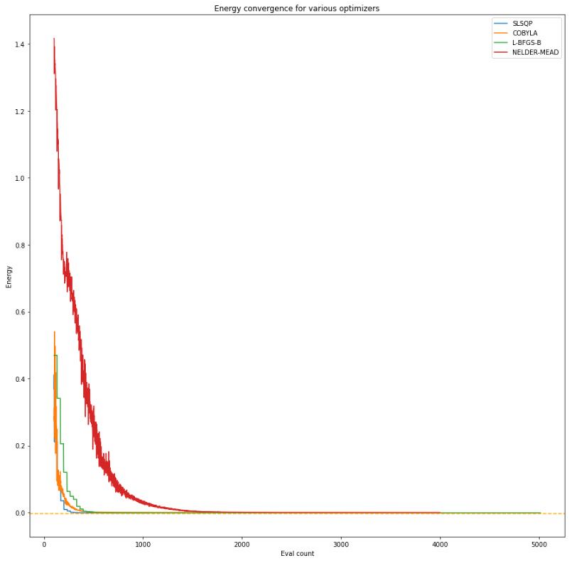

Figure 7: VQE convergence plot for the Hamiltonian with $\Lambda = 0$. Each curve represents a different optimizer, listed in the upper right hand corner. The least accurate optimizer was the NELDER-MEAD, while the most accurate was the L-BFGS-B.

The exact eigenvalue result for the $\Lambda = 0$ case is 0. The most accurate VQE result is $1.09036668 * 10^{-10}$, achieved by the L-BFGS-B optimizer.

We did the same VQE run for the mass operator where $\Lambda = 0$, in Figure 8.

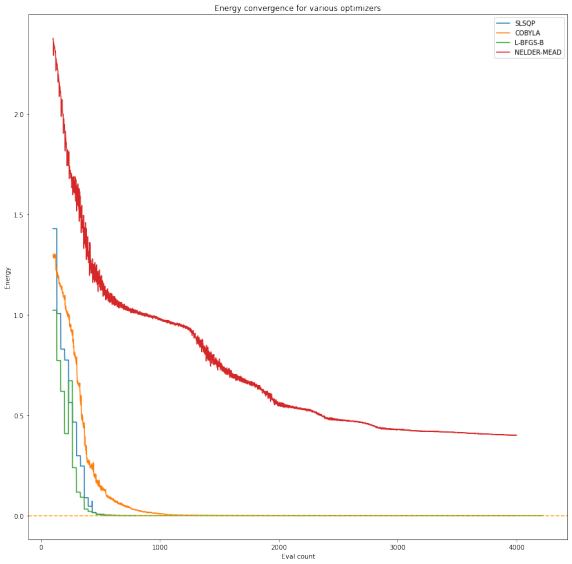

Figure 8: VQE convergence plot for the mass operator with $\Lambda = 0$. Each curve represents a different optimizer, listed in the upper right hand corner. The least accurate optimizer was the NELDER-MEAD, while the most accurate was the L-BFGS-B.

The exact result for the mass operator is $-5.25243013 * 10^{-16}$ and the most accurate VQE result is $6.4310571512 * 10^{-08}$.

For non-zero lambda, we used $\Lambda = 3$, rather than its observed value, for illustrative purposes in order to study the effect of dS space. The actual value for the cosmological constant is on the order of 10^{-120} in natural units where Newton's constant $G = 1$.

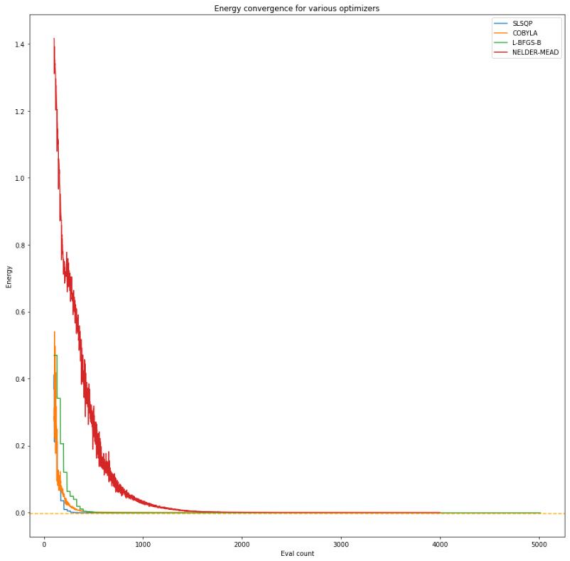

Figure 9: VQE convergence plot for the Hamiltonian with $\Lambda = 3$. Each curve represents a different optimizer, listed in the upper right hand corner. Similar to the zero lambda case, the least accurate optimizer was the NELDER-MEAD, while the most accurate was the L-BFGS-B.

The evaluated exact value for non-zero lambda is -0.00311036 while the VQE result gave -0.001139438879178998 (with the L-BFGS-B optimizer). The approximate error for the non-zero lambda VQE result is 63.36%, which is fairly large.

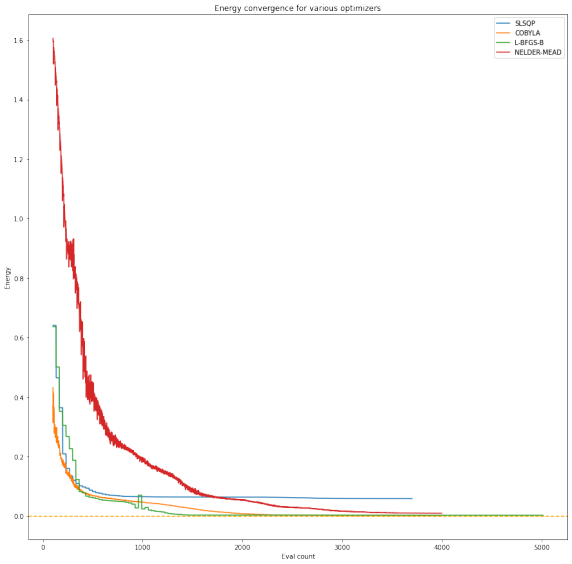

Figure 10: VQE convergence plot for the mass operator with $\Lambda = 3$. Each curve represents a different optimizer, listed in the upper right hand corner. The least accurate optimizer was the SLSQP (blue), while the most accurate was the COBYLA (orange).

The exact value is $7.88618159 * 10^{-16}$, whereas the most accurate VQE result is 0.001809337379032537, which was actually from the COBYLA optimizer.

It should be noted that we did run the VQE at larger qubits, creating a 256 by 256 matrix (with the Kronecker product) which led to less accurate results that took significantly longer to run.

Finally, the evolution of the Hamiltonian (EOH). The EOH describes how the energy states of the system evolve over time. In order to evolve it through time, we can use the equation,

$$e^{-iHt}$$

We use the quantum computer to plot the evolution using the finite difference basis and the position basis, shown in Figures 11 and 12, respectively.

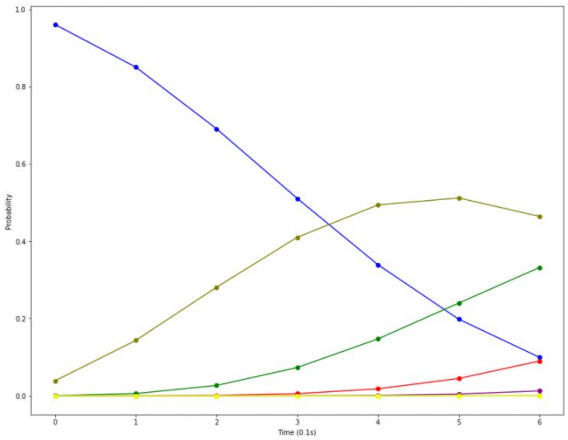

Figure 11: Plot of the evolution of the Hamiltonian in the finite difference basis.

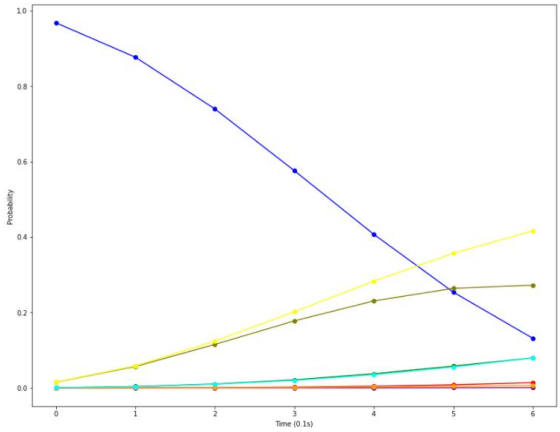

Figure 12: Plot of the evolution of the Hamiltonian in the position basis.

Each curve in the plots represents a different energy state's probability throughout time. Since it is given as probabilities, the total for a given time is equal to 1. The plots show the EOH for the interior of the black hole is very similar to that of the simple harmonic oscillator.

6 Thermofield Double

Recall that black holes have been shown by Hawking and Gibbons to be thermodynamical systems. Thus, we can study how they evolve in temperature (rather than

time as in the EOH).

The thermofield double (TFD) is a special entanglement state that cannot be denoted by a mixture of states. It is a way to study a thermal system by introducing a "double" particle (in our case, boson) into the TFD state [10]. The method is useful in the study of event horizons as it involves an entanglement of two bosons which can be placed on either side of the black hole even horizon [10]. The equations found in [11] define,

$$G = -i\left(\tilde{a}a - a^{\dagger}\tilde{a}^{\dagger}\right)$$
$$\theta(\beta) = \operatorname{arctanh}\left(e^{-\beta\omega/2}\right)$$
$$\theta(\beta) = \frac{1}{kT}$$

where a and $\tilde{a}$ are the raising operators for the boson and its double. They can be constructed by taking the Kronecker product with the identity matrix. Note that we only need bosons for the black hole study. β is inversely related to the temperature, so when we plot $\theta(\beta)$ as a function of this inverse temperature we get Figure 13,

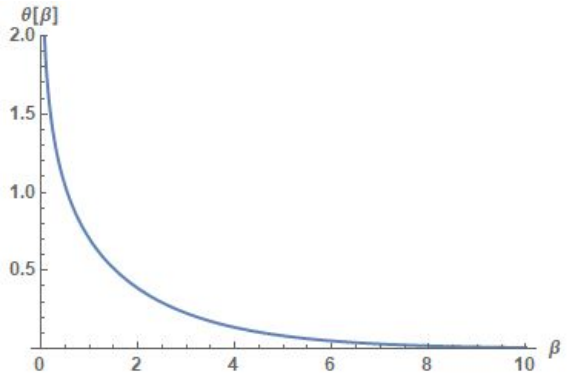

Figure 13: Plot of $\theta(\beta)$ as a function of $\beta = \frac{1}{T}$ (set the Boltzmann constant equal to 0). We can see the function decrease at a decreasing rate, approaching 0.

When we study the TFD state, it is similar to the evolution of the Hamiltonian except that we evolve in temperature rather than time and use the defined G instead of the Hamiltonian. Thus, to evolve in temperature we use,

$$e^{-i\theta G}$$

We derive the probabilities of each evolution state and plot them using Mathematica. These are called the Boltzmann probabilities,

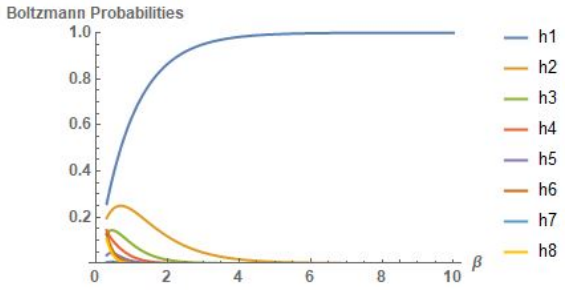

Figure 14: Plot depicting the evolution of the thermofield double. It is the Boltzmann probabilities as a function of inverse temperature. Each curve represents the probability of the TFD existing in that state.

We can also plot the TFD using the quantum computer, following the same process, in Figure 15.

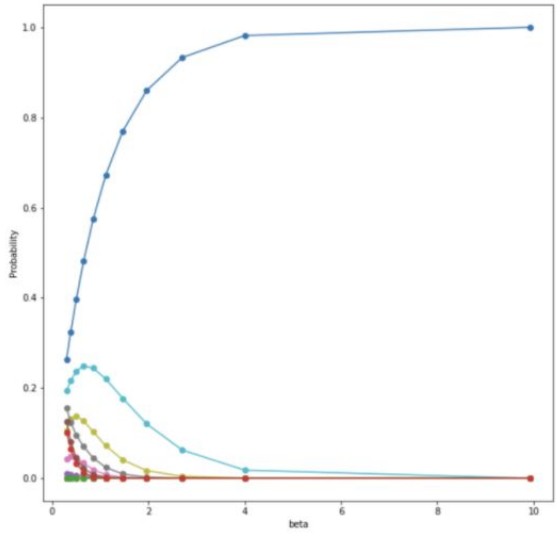

Figure 15: Plot depicting the evolution of the thermofield double over temperature. Again, it's the Boltzmann probabilities as a function of inverse temperature. Each curve represents the probability of the TFD existing in that thermal state.

Notice the quantum computer was able to accurately keep up with the classical computer's calculations - both plots look very similar and prove the TFD's evolution in temperature.

The TFD is an important concept to include when studying black holes and

cosmology. It allows for the conceptualization of the classically odd features of a black hole, particularly allowing for the entanglement of two particles near the event horizon surface.

7 Conclusion

The Schwarzschild-de Sitter solution to Einstein's equation is a useful application to tie black holes and the Universe together. The two seemingly different concepts have vital similarities that can be interesting to explore. One idea that appears is the Nariai solution - the largest possible de Sitter black hole. Perhaps, the most intriguing quality of the Nariai black hole is that it has no spacial singularity, but rather a singularity in time. This is contrary to other peculiarities such as extremal black holes or the Universe itself which have naked singularities. For further research, it would be of interest to continue to investigate this oddity and the Nariai solution as whole in more detail. Additionally, the EOH and TFD provide compelling information about how the energy and thermal states evolve over time and temperature. The quantum computer was accurate in its replications of the classical computer's calculations in all areas of this study. It should be noted that as the number of qubits increased, the accuracy actually decreased and the time to run the code increased significantly. This shows the abilities of quantum computers still have a long way to improve. They will be excellent tools for the future of science and technology.

8 Acknowledgements

Thank you to Dr. McGuigan for allowing me to work with him again during this summer and continue our research progress. I appreciate all of the support, guidance, and knowledge shared. This project was supported in part by the U.S. Department of Energy, Office of Science, Office of Workforce Development for Teachers and Scientists (WDTS) under the Science Undergraduate Laboratory Internships Program (SULI).

References

[1] "A Simplified Guide to De Sitter and Anti-De Sitter Spaces." Student Friendly Quantum Field Theory: Basic Principles and Quantum Electrodynamics, by Robert D. Klauber, Sandtrove Press, 2018.

[2] Bousso, Raphael. "Adventures in de Sitter Space." ArXiv.org, 17 May 2002, arxiv.org/abs/hep-th/0205177v1.

[3] Shankaranarayanan, S. "Temperature and Entropy Of Schwarzschild-De Sitter Space-Time." ArXiv.org, 13 Apr. 2003, arxiv.org/abs/gr-qc/0301090v2.

[4] Fernando, Sharmanthie. "Nariai Black Holes with Quintessence." ArXiv.org, 21 Aug. 2014, arxiv.org/abs/1408.5064.

[5] M. Cavaglia, V. de Alfaro and A. T. Filippov, "Hamiltonian formalism for black holes and quantization," Int. J. Mod. Phys. D **4**, 661-672 (1995) doi:10.1142/S0218271895000442 [arXiv:gr-qc/9411070 [gr-qc]].

[6] Maloney, Alexander, et al. "de Sitter Space in Non-Critical String Theory." ArXiv.org, 20 June 2002, arxiv.org/abs/hep-th/0205316.

[7] Obied, Georges, et al. "de Sitter Space and the Swampland." ArXiv.org, 17 July 2018, arxiv.org/abs/1806.08362.

[8] Wiltshire, D. L. "Wave Functions for Arbitrary Operator Ordering in the de Sitter Minisuperspace Approximation." ArXiv.org, 24 May 1999, arxiv.org/abs/gr-qc/9905090.

[9] Miceli, Raffaele, and Michael McGuigan. "Thermo Field Dynamics on a Quantum Computer." ArXiv.org, 8 Nov. 2019, arxiv.org/abs/1911.03335.

[10] Cottrell, W., Freivogel, B., Hofman, D.M. et al. How to build the thermofield double state. J. High Energ. Phys. 2019, 58 (2019). https://doi.org/10.1007/JHEP02(2019)058.

[11] Das, Ashok. Supersymmetry and Finite Temperature. lib-extopc.kek.jp/preprints/PDF/1988/8811/8811283.pdf.

[12] Jalalzadeh, Shahram, and Babak Vakili. "Quantization of the Interior Schwarzschild Black Hole." ArXiv.org, 14 Sept. 2011, arxiv.org/abs/1108.1337.

[13] Curiel, Erik. "Singularities and Black Holes." Stanford Encyclopedia of Philosophy, Stanford University, 27 Feb. 2019, plato.stanford.edu/entries/spacetime-singularities/NakeSingCosmCensHypoInde.

[14] Shaikh, Absos Ali, and Dhyanesh Chakraborty. "On Curvature Properties Of Nariai Spacetimes." ArXiv.org, 20 Aug. 2019, arxiv.org/abs/1902.03918.

[15] Djordjevic, Goran S., et al. "Two-Oscillator KANTOWSKI-SACHS Model of the Schwarzschild Black Hole Interior." ArXiv.org, 4 Oct. 2015, arxiv.org/abs/1510.00887.

[16] Emparan, Roberto, and Harvey S Reall. "Black Holes in Higher Dimensions." Living reviews in relativity vol. 11,1 (2008): 6. doi:10.12942/lrr-2008-6

[17] Eguchi, Tohru, et al. "Gravitation, Gauge Theories and Differential Geometry." Physics Reports, North-Holland, 19 Sept. 2002, www.sciencedirect.com/science/article/abs/pii/0370157380901301.

[18] Hartong, J. "On Problems in De Sitter Spacetime Physics." Inspire, 5 July 2004, inspirehep.net/files/dd379b79a6b1266fcbaba060386d64c6.

[19] Fischler, W., et al. Quantization of False Vacuum Bubbles: A Hamiltonian Treatment of Gravitational Tunneling. libextopc.kek.jp/preprints/PDF/1990/9005/9005428.pdf.